

# EDTN 201

## Initial Evaluation of Haas Super Mini Mill S/N 40150

NRAO PO 207121

A. R. Kerr, A. Marshall, M. Meek, D. Parker, J. Shelton

Rev. 2a 28 Sep 2005

### 1. Introduction

Test pieces made with Haas mill suggest the machine does not meet its  $\pm 200 \mu\text{in}$  position accuracy specification in the Y direction. Although the Haas engineer who installed the machine thought it was behaving atypically in the Y direction and suggested changing the Y-axis servo, Haas say they will not accept measurements made on cut metal test pieces, but only measurements of the table motion relative to the spindle made using a ball bar or laser. Ball bar measurements made by Haas during installation were, reportedly, within spec., but Haas have not yet been able to provide copies of those measurements — it appears they may have been lost when a laptop computer was upgraded.

This memo describes measurements made to date on the Haas machine in an effort to support our machined test piece results. Initial measurements using the Green Bank HP laser interferometer did not indicate that the machine was outside specifications over small distances such as those measured on our test pieces, although it does appear to have excessive position error over distances of several inches. However, as the sequence of machine movements in the laser tests was different from that when machining the test piece, additional laser measurements are indicated.

### 2. Machined Test Pieces

The test pattern shown in Fig. 1 was machined in type 360 free machining brass. All channels are nominally 0.050" wide x 0.050" deep. After roughing with a 0.040" end mill, finishing cuts were made with a 0.031" end mill. The tool path was chosen so all walls of the channels were climb-cut (this has been found to give the best wall quality). Five test pieces were made using different spindle speeds and feed rates:

1. As shown in Fig. 1. Spindle speed 8000 RPM, feed rate 4"/min.
2. Test piece 1 with a final 2 mil surface trim to remove any distortion near the top of the channel. The trimming cut followed the perimeter of the channels, always climb-cutting, to remove burrs.
  - A. Same as test piece 1 but 5000 RPM and 4"/min.
  - B. Same as test piece 1 but 8000 RPM and 2"/min.
  - C. Same as test piece 1 but 4000 RPM and 2"/min.

The widths of all channels were measured on an Olympus STM-UM measuring microscope with digital readouts (glass scales) and 50  $\mu\text{in}$  resolution.

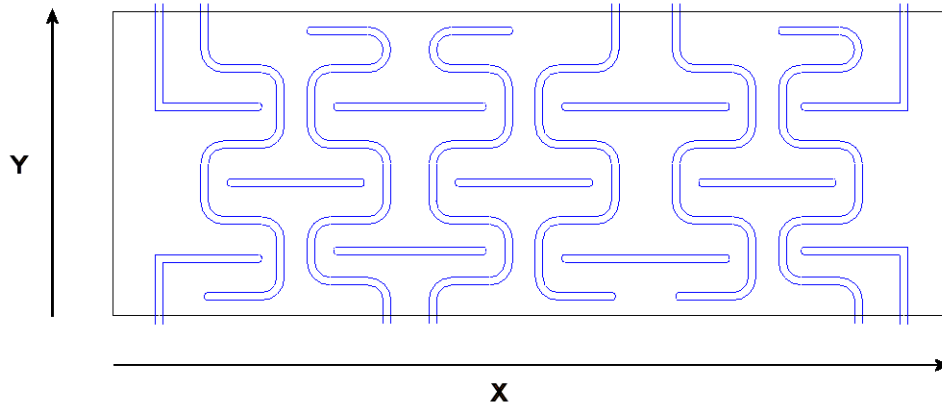


**Fig. 1. Test pattern.**

**Test Piece 1:** Tables I and II show the X-direction and Y-direction measurements, mapped according to their locations in Fig. 1. Also shown in the tables are the deviations of the channel widths from the mean width. Deviations in width greater than  $200\ \mu\text{in}$  are marked in orange and deviations less than  $-200\ \mu\text{in}$  are marked in blue. The X and Y deviations are plotted in histograms in Figs. 2 and 3, which show the number of channels whose width falls in each  $50\text{-}\mu\text{in}$  range (bin) around the mean.

The histogram of the X-direction data, Fig. 2, shows a bell-shaped distribution of channel widths, all within a range of  $400\ \mu\text{in}$ , which is consistent with the machine's specified position accuracy of  $\pm 200\ \mu\text{in}$ . The channel widths in the Y direction, Fig. 3, are distributed over  $650\ \mu\text{in}$ , considerably greater than the  $\pm 200\ \mu\text{in}$  position accuracy of the machine, and have a decidedly double-peaked distribution with the peaks near the ends.

**Test Pieces 2, A, B, and C:** Figs. 4-7 show the Y-direction channel width distributions for test pieces 2, A, B, and C.

**TABLE I — TEST PIECE 1 — X-DIRECTION**

**Measured Channel Width**

Mean = 0.04926"

	0.04930							0.04941		0.04930										0.04945	
0.04930			0.04925	0.04925				0.04920	0.04930				0.04940	0.04910							
	0.04910					0.04910	0.04920					0.04925	0.04910							0.04915	
			0.04930	0.04930				0.04905	0.04930						0.04925						
0.04945						0.04920	0.04940									0.04910		0.04930			0.04940

**Deviation from Mean Width**

Min = -0.00021"

Max = 0.00019"

	0.00004									0.00015		0.00004									0.00019	
0.00004			-0.00001	-0.00001				-0.00006	0.00004				0.00014	-0.00016								
	-0.00016					-0.00016	-0.00006					-0.00001	-0.00016								-0.00011	
			0.00004	0.00004				-0.00021	0.00004													
0.00019						-0.00006	0.00014									-0.00016		0.00004			0.00014	

Deviations >200 µin are marked in orange and deviations < -200 µin are marked in blue.

**TABLE II — TEST PIECE 1 — Y-DIRECTION**

**Measured Channel Width**

Mean = 0.04931

				0.04955				0.04940												0.04955	
		0.04915			0.04900			0.04930			0.04900		0.04920							0.04905	0.04935
	0.04955					0.04955				0.04900		0.04955		0.04920						0.04960	
		0.04905			0.04950			0.04900			0.04950			0.04905						0.04960	
			0.04955						0.04960						0.04950					0.04960	
		0.04920			0.04900			0.04910			0.04900			0.04920						0.04905	0.04965
	0.04925					0.04950						0.04945									0.04965
		0.04925			0.04955			0.04900			0.04945			0.04925						0.04945	

**Deviation from Mean Width**

Min = -0.00031"

Max = 0.00034"

				0.00024				0.00009													0.00024	
		-0.00016			-0.00031			-0.00001			-0.00031			-0.00011							-0.00026	
	0.00024					0.00024						0.00024									0.00004	
		-0.00026			0.00019			-0.00031			0.00019			-0.00026							0.00029	
			0.00024						0.00029						0.00019						-0.00026	
		-0.00011			-0.00031			-0.00021			-0.00031			-0.00011							-0.00026	
		-0.00006				0.00019						0.00014										0.00034
		-0.00006			0.00024			-0.00031			0.00014			-0.00006						0.00014		

Deviations >200 µin are marked in orange and deviations < -200 µin are marked in blue.

### Test Piece 1 -- X-DIRECTION

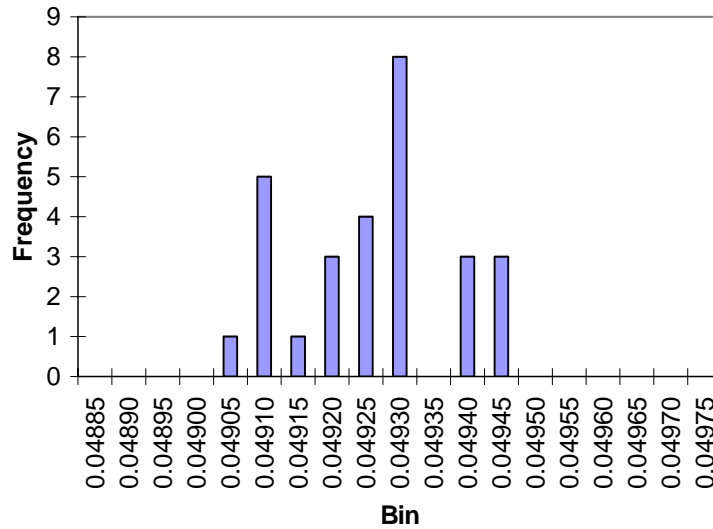


Fig. 2. For test piece 1, the number of channels whose width in the X-direction falls in each 50- $\mu$ m range (bin) around the mean.

### Test Piece 1 -- Y-DIRECTION

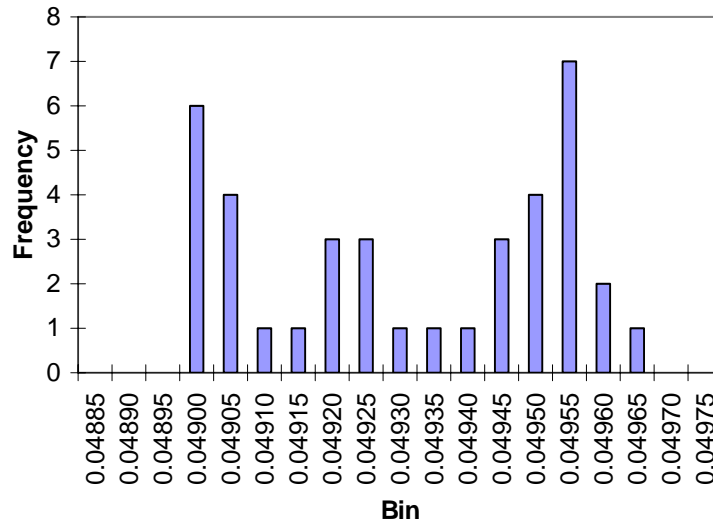


Fig. 3. For test piece 1, the number of channels whose width in the Y-direction falls in each 50- $\mu$ m range (bin) around the mean.

### Test Piece 2 -- Y-DIRECTION

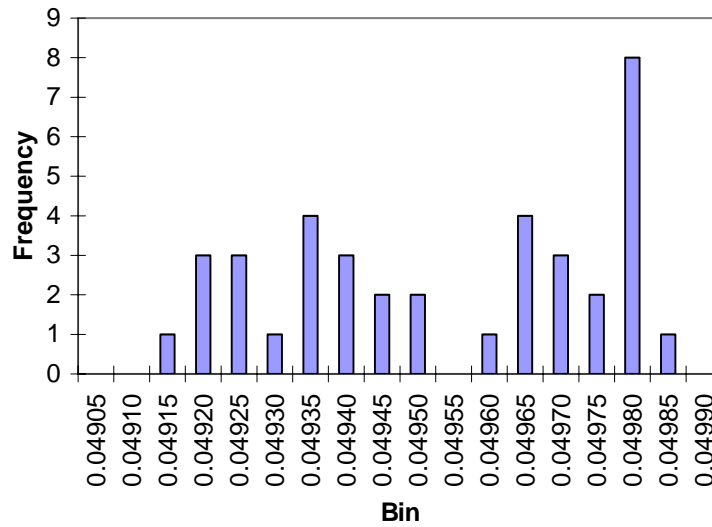


Fig. 4. For test piece 2, the number of channels whose width in the Y-direction falls in each 50- $\mu$ m range (bin) around the mean.

### Test Piece A -- Y-DIRECTION

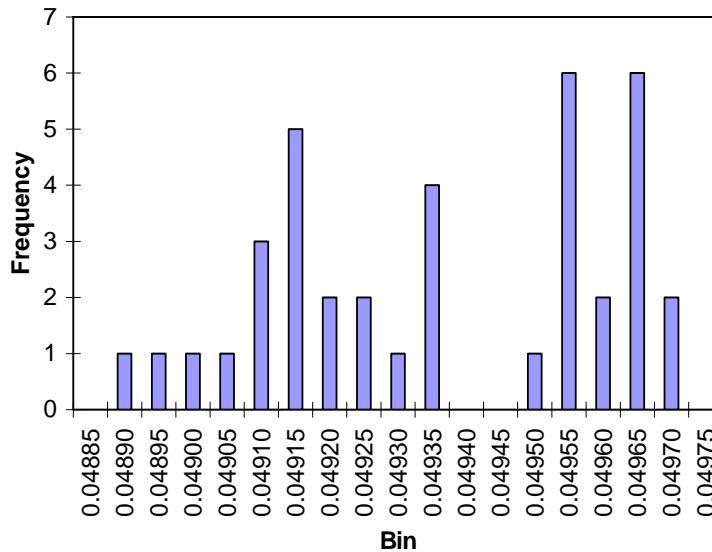


Fig. 5. For test piece A, the number of channels whose width in the Y-direction falls in each 50- $\mu$ m range (bin) around the mean.

### Test Piece B -- Y-DIRECTION

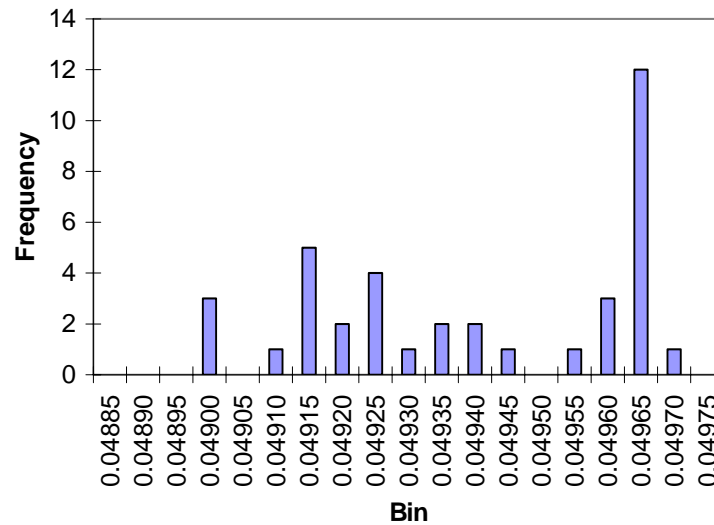


Fig. 6. For test piece B, the number of channels whose width in the Y-direction falls in each 50- $\mu$ m range (bin) around the mean.

### Test Piece C -- Y-DIRECTION

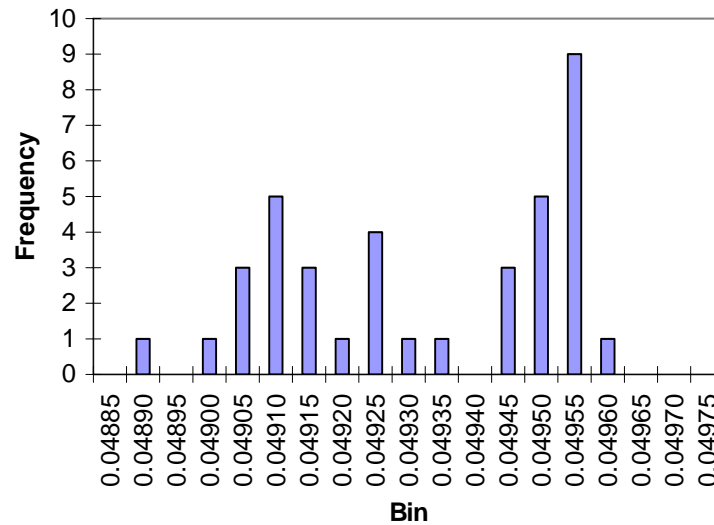


Fig. 7. For test piece C, the number of channels whose width in the Y-direction falls in each 50- $\mu$ m range (bin) around the mean.

### 3. Laser Interferometer Measurements

Measurements were made on the Haas mill using the Green Bank HP 5508A laser interferometer. This instrument has a resolution of  $10\ \mu\text{in}$  and is stable to less than  $10\ \mu\text{in}$ . The beam from the laser (Fig. 8) passes through a combined beam splitter and retroreflector attached to the table of the mill (Fig. 9). Part of the beam is reflected back to the laser unit and part of it is transmitted to a second retroreflector mounted on the spindle of the mill where it too is reflected back into the laser unit. The interferometer readout (Fig. 10) indicates the distance between the two retroreflectors.

The photographs show the setup for measuring the X-axis of the mill. Y-axis measurements are set up similarly, with the laser beam entering the mill through the door of the housing.



**Fig. 8** Laser unit of the HP interferometer as set up for measuring the X-axis. The laser beam enters the mill through a small hole in right cover.



**Fig.9** Setup for the X-axis measurements. The beam splitter and retroreflector are at the right on the table of the mill. The retroreflector at the left is attached to the spindle.



**Fig. 10** Interferometer read-out.

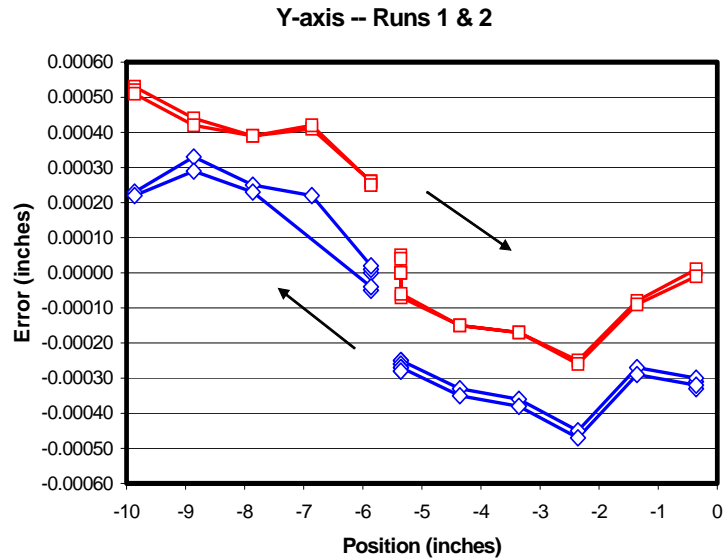


**Fig. 11 Position error vs Y-axis position, two scans in each direction. Red points are for increasing Y, blue points for decreasing Y.**

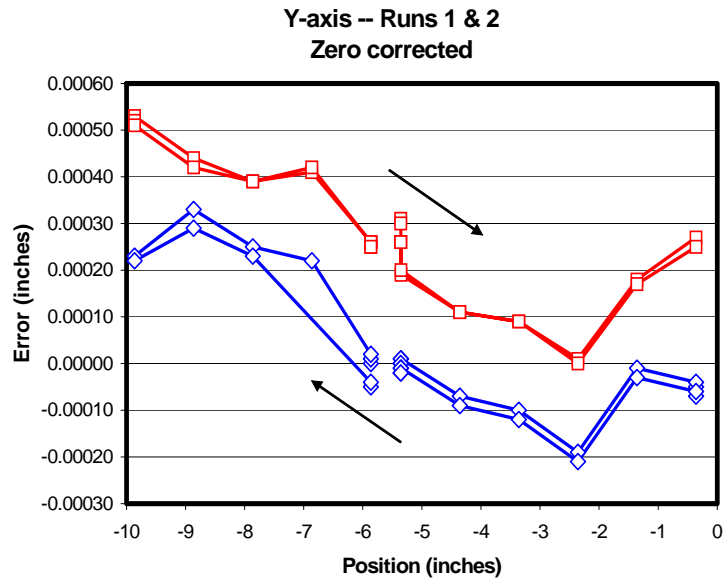


**Fig. 12 Position error vs Y-axis position. The data are the same as in Fig 7, but with the zero misalignment removed (see text). Red points are for increasing Y, blue points for decreasing Y.**

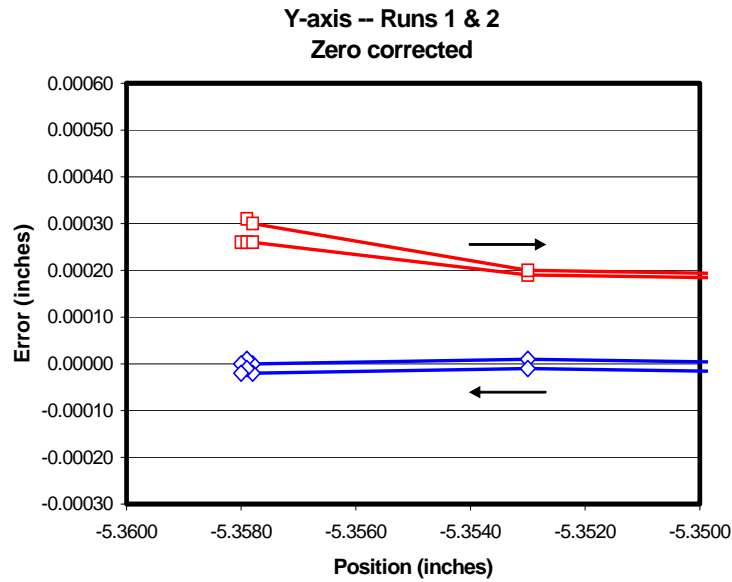
Figure 11 shows the measured position accuracy of the mill in the Y direction. To prevent the two retroreflectors colliding, two setups were used, one for  $Y < -5.5''$  and the other for  $Y > -5.5''$ . The zero positions for the two sets of measurements were set with the table approaching from opposite directions; this accounts for the vertical offset between two sets of data in Fig. 11. In



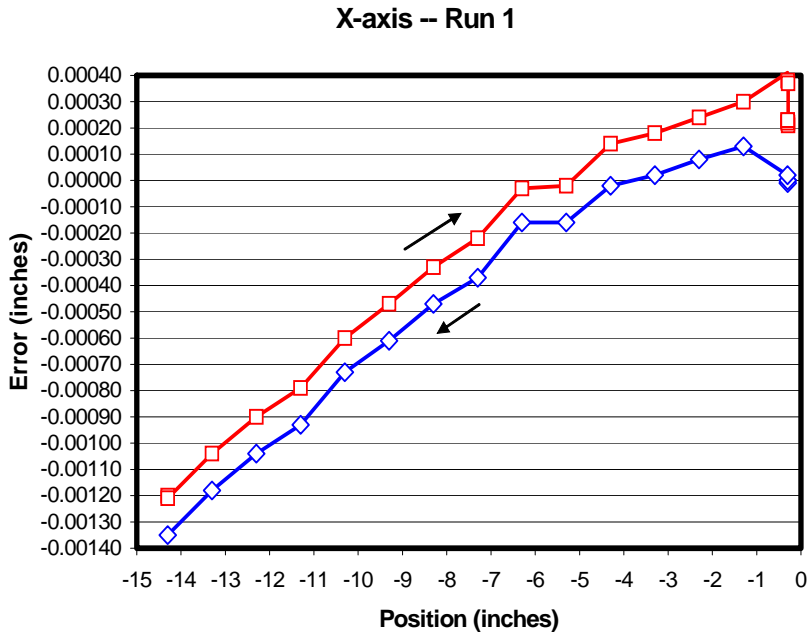
Fig. 12, the same data are re-plotted with this zero discrepancy removed. The apparently vertical grouping of several points near  $Y = -5.355$ " is expanded in Fig. 13.

Figure 14 shows the measured position accuracy of the mill in the Y direction. The apparently vertical grouping of several points near  $X = -0.300$ " is expanded in Fig. 15.

Figure 16 shows details of hysteresis in the X-axis. Similar results were obtained near  $X = -0.300$ ",  $-4.300$ ",  $-8.3$ ",  $-12.3$ ", and  $-14.3$ ".



**Fig. 13 Data of Fig. 12 expanded about  $Y = -3.355$  to explain the apparently vertical grouping of several points in Figs. 11 and 12.**



**Fig. 14** Position error vs X-axis position, two scans in each direction. Red points are for increasing X, blue points for decreasing X.

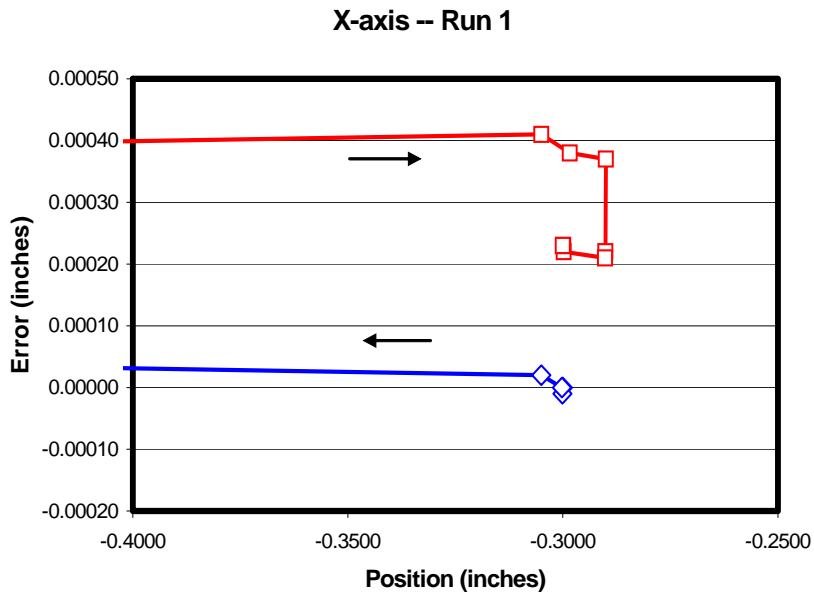


**Fig. 15** Data of Fig. 14 expanded about X = -0.30 to show the details of the apparently vertical grouping of several points.

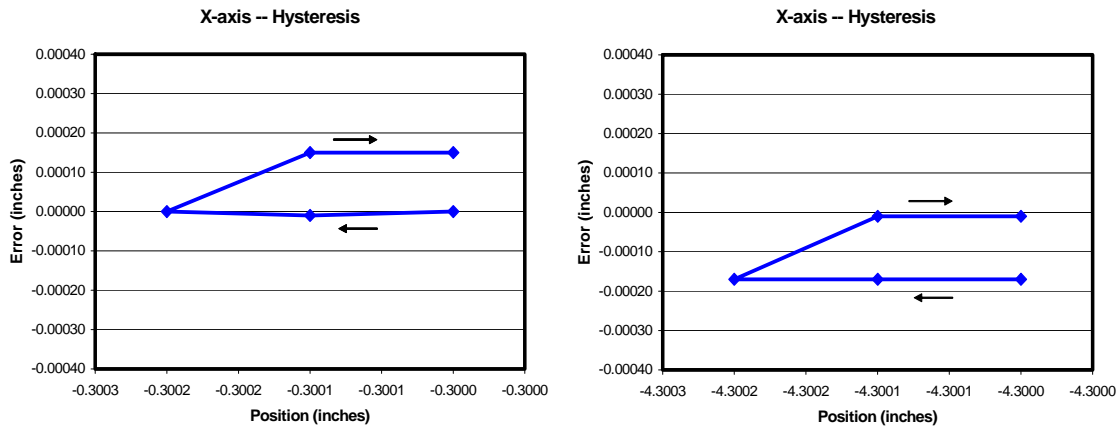


**Fig. 16 Details of X-axis hysteresis near X = -0.300" and -4.300". Similar results were obtained at X = -8.300", -12.300", and -14.300".**

#### 4. Discussion

The wide distribution of channel widths,  $\pm 320 \mu\text{in}$ , in the Y-direction on all five of the machined test pieces, Figs. 3-7, is considerably beyond the  $\pm 200 \mu\text{in}$  position accuracy specification of the Haas mill. For comparison, channel widths in the X-direction, Fig. 2, were within  $\pm 200 \mu\text{in}$  as expected. It was expected that the Y-axis results would be reflected in the laser interferometer measurements, but they were not. The laser measurements of the Y-axis motion in Fig. 5 indicate excellent repeatability, within less than  $40 \mu\text{in}$ , when the motion is in the same direction. When the direction of motion is reversed, hysteresis or backlash is observed, but the Y position is within  $200 \mu\text{in}$ . For the X axis, hysteresis was also within  $200 \mu\text{in}$  except at a few points on the right in Fig. 10, where it is within  $400 \mu\text{in}$  (*i.e.*, within the  $\pm 200 \mu\text{in}$  spec.).

Over relatively large distances, typically  $> 6"$ , the position accuracy measured with the laser interferometer was outside the specified  $\pm 200 \mu\text{in}$ . In the Y direction, from Fig. 12, the ingoing position at Y = -10 is off by  $700 \mu\text{in}$  relative to the outgoing position at Y = -2.3. In the X direction, from Fig. 14, the ingoing position at X = 0 is off by  $1,700 \mu\text{in}$  relative to the outgoing position at X = -14.

The measurements were made with the machine at  $\sim 72^\circ \text{F}$  ( $22^\circ \text{C}$ ). To calculate whether temperature changes might explain the position error over long distances, an expansion coefficient of  $12 \times 10^{-6} / ^\circ \text{C}$  was assumed for steel. A temperature change of  $8.3^\circ \text{C}$  ( $15^\circ \text{F}$ )

would be required to cause an expansion of 0.0014" over 14". It therefore seems unlikely that thermal expansion is the main cause of the long-distance position errors.

Note that, in both X and Y directions, the hysteresis is negative, *i.e.* the table position does not lag behind the commanded position, as one would expect if there were simple backlash in the ballscrew and nut, but is actually ahead of the commanded position. We surmise that the internal software of the machine senses the direction of motion and over-compensates for backlash, perhaps in an effort to accommodate wear as the machine ages.

While the laser measurements indicate that the Haas mill is out of spec in its position accuracy when measured over distances of more than 6", nothing was seen in the Y-axis laser measurements that would explain the width errors measured on the channels in our test piece. However, with the setup used in these measurements, the laser interferometer was not able to do measurements while the machine followed the tool path used for the test pieces.

## 5. Recommendations

The laser interferometer should be used to measure the motion of the machine while it follows the same tool path used for the test pieces.